Barrier Permeability at Cut Axonal Ends Progressively Decreases until an Ionic Seal Is Formed

Christopher S. Eddleman,*[†] George D. Bittner,*[‡§¶] and Harvey M. Fishman*

*Department of Physiology and Biophysics, University of Texas Medical Branch, Galveston, Texas 77555-0641; [†]Texas Tech University Health Sciences Center, School of Medicine, Lubbock, Texas 79430; [‡]School of Biological Sciences, Neurobiology Section, [§]College of Pharmacy, and [¶]Institute for Neuroscience, The University of Texas at Austin, Austin, Texas 78712 USA

ABSTRACT   After axonal severance, a barrier forms at the cut ends to rapidly restrict bulk inflow and outflow. In severed crayfish axons we used the exclusion of hydrophilic, fluorescent dye molecules of different sizes (0.6–70 kDa) and the temporal decline of ionic injury current to levels in intact axons to determine the time course (0–120 min posttransection) of barrier formation and the posttransection time at which an axolemmal ionic seal had formed, as confirmed by the recovery of resting and action potentials. Confocal images showed that the posttransection time of dye exclusion was inversely related to dye molecular size. A barrier to the smallest dye molecule formed more rapidly (<60 min) than did the barrier to ionic entry (>60 min). These data show that axolemmal sealing lacks abrupt, large changes in barrier permeability that would be expected if a seal were to form suddenly, as previously assumed. Rather, these data suggest that a barrier forms gradually and slowly by restricting the movement of molecules of progressively smaller size amid injury-induced vesicles that accumulate, interact, and form junctional complexes with each other and the axolemma at the cut end. This process eventually culminates in an axolemmal ionic seal, and is not complete until ionic injury current returns to baseline levels measured in an undamaged axon.

INTRODUCTION

At a site of axolemmal damage the rapid formation of a barrier, which eventually becomes an ionic seal that restricts the movement of molecules and ions to levels found in intact axons, is essential for the repair of an injured axon (Bittner and Fishman, 2000). A barrier to hydrophilic fluorescent dye, as measured optically by the exclusion of a dye placed in the physiological solution bathing an axon or the containment of dye placed in the axoplasm, forms amid an accumulation of vesicles at the site of axolemmal damage (Eddleman et al., 1997, 1998a; Ballinger et al., 1997; Blanchette et al., 1999; Lichstein at al., 2000). A barrier to ionic movement, as measured electrically by the decline of ionic injury-current density (I_i) to baseline levels found in intact axons and the return of resting membrane potential (E_r) to values in uninjured axons, also forms at the site of axolemmal damage (Krause et al., 1994; Eddleman et al., 1997; Godell et al., 1997). However, barriers assessed by dye exclusion appeared to form earlier than barriers assessed by decay of I_i (Ballinger et al., 1997). These preliminary data raised questions as to whether optical versus electrical measures assessed the same barriers and whether the permeability of any such barrier(s) to ions and larger molecules changed with time.

We now report that confocal, fluorescence images of extracellularly placed hydrophilic dye molecules of different sizes and measures of I_i and E_r show that molecular inflow and outflow at the cut end of severed crayfish medial giant axons (MGAs) continuously decrease with posttransection time. That is, a barrier at the cut end to the largest dye molecule forms first, followed by the progressive restriction of the movement of smaller dye molecules, and finally, upon completion of a seal, restriction of ionic movements at the cut end equivalent to that found across an undamaged axolemma in control, intact axons. Furthermore, a barrier to any given molecule does not form instantaneously, but rather occurs gradually over time. When combined with our previous observations (Krause et al., 1994; Eddleman et al., 1997, 1998a, b; Blanchette et al., 1999; Lichstein et al., 2000), these data suggest that the vesicles that accumulate at a site of axolemmal damage interact to form a barrier that progressively restricts the movement of smaller and smaller molecules between the intracellular and extracellular fluids. Eventually, an ionic seal (Bittner and Fishman, 2000) is formed when I_i is restored to the level measured in an uninjured axon.

MATERIALS AND METHODS

Preparations

Crayfish (*Procambarus clarkii*) ~2–3 inches in body length (Atchafalaya Biological Supply, Raceland, LA), were anesthetized on ice for 5–10 min. The ventral nerve cord (VNC) containing the paired MGAs was removed from the animal, as described previously (Eddleman et al., 1997), and bathed in a physiological saline (van Harreveld, 1936). MGAs were isolated and finely cleaned by carefully teasing away connective and other surrounding tissue with minutien pins (Janni Butterfly Enterprises, Cleveland, OH). Damaged MGAs that had injury-induced vesicles or opaque regions were discarded. Undamaged MGAs were transected with microdissection scissors, as described previously (Eddleman et al., 1997).

Crayfish physiological saline (vanH solution) consisted of the following (in mM): 205 NaCl, 5.4 KCl, 2.6 $MgCl_2$, 13.5 $CaCl_2$, and 10.0 HEPES, pH

7.4. Divalent-cation-free vanH was composed of the following: 205 NaCl, 5.4 KCl, 10.0 HEPES, 24.15 TMA-Cl, 1.0 EGTA, and 1.0 EDTA, pH 7.4. Calcium-free vanH was composed of the following: 205 NaCl, 5.4 KCl, 10.0 HEPES, 2.6 MgCl$_2$, 22 TMA-Cl, 1.0 EGTA, and 1.0 EDTA, pH 7.4. The osmolality of all prepared solutions was measured with an osmometer (Model 5100, Wescor Inc., Logan, UT). The osmolality of vanH solution was ~424 mOsm/l. All other crayfish salines were adjusted to this value. In experiments that required blockage of conduction in axolemmal ion channels (Narahashi, 1974), the following agents (abbreviation: specific channel, source) were used: tetrodotoxin (TTX: Na$^+$, Calbiochem, La Jolla, CA, cat. 554412); tetraethylammonium chloride (TEA: K$^+$, Sigma-Aldrich, St. Louis, MO, cat. T2265); 4-aminopyridine (4-AP: K$^+$, Sigma-Aldrich, cat. A134); nitrendipine (Ca^{2+}, Sigma-Aldrich, cat. N144).

Isolated (intact) MGAs (80–150 μm in diameter) are surrounded by a 3- to 10-μm-thick nonmyelinated glial sheath in which layers of glial processes alternate with extracellular matrix containing collagen (Ballinger and Bittner, 1980; Eddleman et al., 1997).

Confocal microscopy and fluorescent dye molecules as probes of axolemmal integrity

Axons were viewed in vitro with a laser-scanning confocal microscope (LSM 410 or 510, Carl Zeiss, Inc.) equipped with differential interference contrast (DIC) optics, Zeiss Achroplan objective lenses [40× water immersion (NA = 0.75, WD = 1.9 mm) and 63× water immersion (NA = 0.9, WD = 1.5 mm)], an Ar/Kr laser (488, 568, 648 nm) and filter sets for fluorescein-dextran and TRITC (tetramethylrhodamine isothiocyanate). Axons were placed on a 0.1-mm-thick glass coverslip that replaced part of the base of a plastic petri dish (~3 ml). Hydrophilic fluorescent dyes (Calcein [excitation/emission wavelength = 494/517 nm] and Texas Red-dextran [595/615 nm]) were obtained from Molecular Probes (Eugene, OR). These dyes are membrane-impermeant and were used to probe axolemmal integrity at various times posttransection by replacement of the vanH solution with vanH containing a dye (added to the solution at 0.01% w/v) composed of molecules of specific size (0.6-kDa Calcein or 3-kDa or 70-kDa Texas Red-dextran).

To maximize the dynamic range of fluorescence intensities determined during line scans of confocal fluorescence images, the contrast and brightness levels were adjusted to maximize the value of fluorescence intensities in the regions where the dye had been placed. These contrast and brightness settings were maintained constant during experiments to ensure that fluorescence intensity levels in all images in each experiment could be compared. To enhance signal-to-noise ratio, each line of a confocal image was usually built up from the average of eight line scans.

To determine dye uptake or exclusion, the fluorescence intensity in a transected axon was compared to its fluorescence level before injury and/or to a paired intact cell. To compare axonal fluorescence intensity levels to the extracellular levels, intensity scans were made along a line that extended from outside, through the cut end, and into the axon. When the change in fluorescence intensity was significant and abrupt (>90% within ±10 μm) from the outside to the inside of the axon along the line scan, a physical barrier to dye entry or exit was assumed to have formed. A similar criterion was used previously to yield assessments that are as reliable as those which use the relative intensities in an intact, uninjured axon as a control to assess whether a dye barrier has formed in a severed axon (Ballinger et al., 1997).

The barrier formation time for the different sizes of dye molecules was assessed in separate axons as follows. At a specific time posttransection, the bath vanH was replaced by vanH containing the test dye of particular molecular size in a modified petri dish containing four or more separate transected axons. Allowing 15 min for dye entry, a line intensity scan was then made, as described above, to assess whether the dye was excluded. From the population of transected axons to which the test dye was added at the same posttransection time, the fraction of the total number of axons that excluded the dye was plotted as a single data point representing the

percentage (%) of axons that excluded the test dye added at the specific posttransection time. This protocol was repeated for the same set of posttransection times for all three dyes of different molecular size and to well beyond the posttransection time (120 min) when all (100%) transected axons excluded each dye.

To determine the size distribution of the molecules in each fluorescent dye used, each dye (0.1% in physiological solution of 0.6-kDa Calcein, and 3-kDa or 70-kDa Texas Red-dextran) was loaded onto separate gels composed of 15, 12, and 10% polyacrylamide, respectively, along with protein standards (ranging in mol size from 2.5 to 200 kDa, Mark 12, Novex, San Diego, CA for 0.6-kDa Calcein and 3-kDa Texas Red-dextran and ranging in mol size from 20.9 to 107 kDa, Bio-Rad, Hercules, CA for 70-kDa Texas Red-dextran). After running for 30 min at 80 VDC using a Bio-Rad Mini-Vertical Electrophoresis System, each gel was stained with Coomassie Blue. The gels were then scanned (Hewlett Packard, Palo Alto, CA, Model 6300C) to produce images that were assembled using software (Adobe, San Jose, CA, Photoshop) to form a composite image in which the lanes were moved vertically until the values of the protein standard markers of mol size for each gel were in the correct position relative to the values of the markers for the other gels.

Assessment of ionic sealing and electrical recovery

The "vibrating probe" technique (Jaffe and Nuccitelli, 1974; Scheffey, 1988) provided a sensitive way to map and record the variation of I_i (ionic injury current density) in the extracellular medium surrounding an injured axon. We determined the magnitude and direction of the I_i vector at any point in the medium from 1) the voltage difference between the limits of the probe tip (3–5 μm in diameter) excursion (a few μm in two dimensions [x and y at constant z]) in the extracellular medium of known electrical conductivity; and 2) the spatial coordinates of the probe tip excursion.

Before transection of each axon, control current density (I_c) was surveyed along an entire length of axon (~1 cm) adjacent to the point where the transection was to be made. The average of a set ($n = 5$) of such determinations was designated as the baseline I_c for that axon, i.e., the control current in the intact, uninjured axon before transection. Axons were rejected from experimentation if an individual determination of I_c at any point along an intact axon exceeded twice the background (noise) current density measured without an axon in the chamber. The ionic sealing time in a given axon was determined by measuring the time required for I_i to decay to the value of I_c determined for that axon before transection.

Measurement artifacts due to movement (contraction) of the preparation were eliminated by continuous video microscopic observations, which allowed us to reposition the probe so that, when acquiring I_i data, we could keep the distance between the probe and the cut end constant (at a fixed distance of 150 μm). To eliminate electrical drift from the I_i determinations, we reestablished the zero injury-current baseline before each sample of I_i by moving the probe tip to a reference position far (>1 cm) from the cut axonal end. After I_i had attained baseline level (I_c), the probe tip was moved successively closer to the cut end to assure that the injury current at the cut end had returned to I_c. To reduce any effects from the vibration of the probe on I_i, between each I_i determination the probe was moved at least 1 mm from the cut end and the vibration was terminated until the next measurement. In a few axons, we delayed sampling I_i with the vibrating probe electrode until 50 min posttransection. In these measurements, the posttransection times at which I_i attained baseline were indistinguishable from those obtained using the above procedures in which we sampled I_i over its entire time course.

To assess recovery of E_r (resting membrane voltage) and action potential propagation after decay of I_i to I_c, MGAs were impaled with glass microelectrodes (10–20 MΩ) filled with 2 M KCl. The E_r was determined before transection, and then the microelectrode was removed to avoid damage (Yawo and Kuno, 1985). After transection, MGAs were impaled at various times from 5 to 120 min at a short distance (50–300 μm) from the

injury site. Axons could be impaled many times without a significant decrease (>1 mV) in the E_r. Propagation of transmembrane action potentials could be measured during microelectrode impalements by extracellular stimulation of an axon by passage of pulses of current through two closely spaced (2 mm separation) platinum wires in contact with the axon surface and located ~1 cm from the point of impalement.

RESULTS

The posttransection time at which hydrophilic dye is excluded from severed axons varies inversely with dye molecular size

We first determined whether severed crayfish MGAs form a barrier to hydrophilic, fluorescent dye molecules of different size added extracellularly at posttransection times ranging from 5 to 120 min. To assure distinct differences in the molecular size of the molecules in each dye (70-kDa, 3-kDa Texas Red-dextran or 0.6- kDa Calcein), we compared their banding patterns on separate electrophoretic gels composed of 10, 12, and 15%, respectively, polyacrylamide along with protein standards (see Materials and Methods). The 0.6- and 3-kDa dyes were homogeneous (produced a single band) with respect to the molecular size of their constituent molecules, whereas the 70-kDa dye produced a heterogeneous band. Nevertheless, the bands produced by all three dyes were well-separated from each other in relation to the molecular sizes of the protein standard markers (Fig. 1), indicating that the dye molecules in each dye were in quite different molecular size ranges. Consequently, the size distribution of the molecules comprising each of the three dyes was sufficiently narrow and separate to allow us to use them as three distinctly different-sized molecular probes.

Dye exclusion (barrier formation) by MGAs transected in crayfish physiological saline (vanH, see Materials and Methods) was assessed from intensity scans of images of fluorescence acquired by confocal microscopy (Fig. 2). For example, when each of the different-sized hydrophilic dye probes (70, 3, or 0.6 kDa) was added to the saline solution bathing separate transected MGAs at 15 min posttransection and a confocal image was acquired 15 min later (Fig. 2, *right*), scans of the fluorescence intensity (Fig. 2, graphs of intensity versus distance) along a line extending from outside to inside each cut end were different. The cut end exposed to the smallest dye molecules (0.6 kDa, *open square*) showed considerable uptake of dye (i.e., interior intensities [20–120 μm from the cut end] were ~50% of the intensity of the dye in the bath). The cut end exposed to the intermediate-sized dye molecules (3 kDa, *closed triangle*) also had taken up the dye, but to a lesser extent (i.e., interior intensities [20–120 μm from the cut end] were ~25% of the intensity of the dye in the bath). In contrast, the cut end exposed to the largest dye molecules (70 kDa, *open circle*), as indicated by the sharp decrease in intensity (within a distance of ±10 μm of the cut end [0 on the *x* axis]) to a constant background level of only 7% of the intensity of the
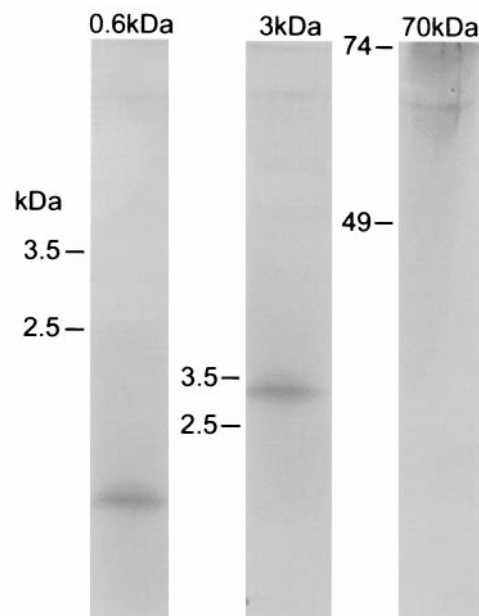

FIGURE 1 Electrophoretic characterization of the hydrophilic fluorescent dyes (0.6, 3, and 70 kDa) used to probe barrier formation at the cut ends of severed axons. Composite image formed by running each dye on a separate polyacrylamide gel of different density together with protein standards (see Materials and Methods). The 0.6- and 3-kDa dyes produced a single band with respect to the molecular size of their constituent molecules, while the 70-kDa dye produced a heterogeneous band. Notice, however, that the distributions of molecular sizes in the three dyes are well-separated, as indicated by the molecular size of the protein standard markers, allowing them to be used as three distinctly different-sized molecular probes.

dye in the bath, showed no dye uptake. That is, at 15 min posttransection, axons had formed a barrier at cut ends that excluded 70-kDa dye molecules, but did not exclude the smaller dye molecules.

When any of the hydrophilic dyes (70, 3, or 0.6 kDa) was added to the saline solution bathing transected MGAs (Fig. 3) at 5 min posttransection, all axons ($n > 20$) took up the dye, i.e., no physical barrier to dye entry was observed. When dye was added to the bath of MGAs at 10 min posttransection, 40% of axons (2 of 5) excluded the 70-kDa dye compared to 0% exclusion of the 3-kDa (0 of 4) or the 0.6-kDa dye (0 of 4). At 15 min posttransection, 67% of axons (4 of 6) excluded the 70-kDa dye and only 10% of axons (1 of 10) excluded the 3-kDa dye, whereas 0% of axons (0 of 4) excluded the 0.6-kDa dye. At 30 min posttransection, 100% (8 of 8) of axons excluded both the 70-kDa and 3-kDa dyes, while 0% of axons (0 of 4) excluded the 0.6-kDa dye. At 40 min posttransection, only 25% of axons (2 of 8) excluded the 0.6-kDa dye, whereas at 50 min posttransection, 83% of axons (5 of 6) excluded the 0.6-kDa dye. These data (Fig. 3) clearly show that the physical barrier that forms during sealing of a severed axon progressively excludes molecules of decreasing size with
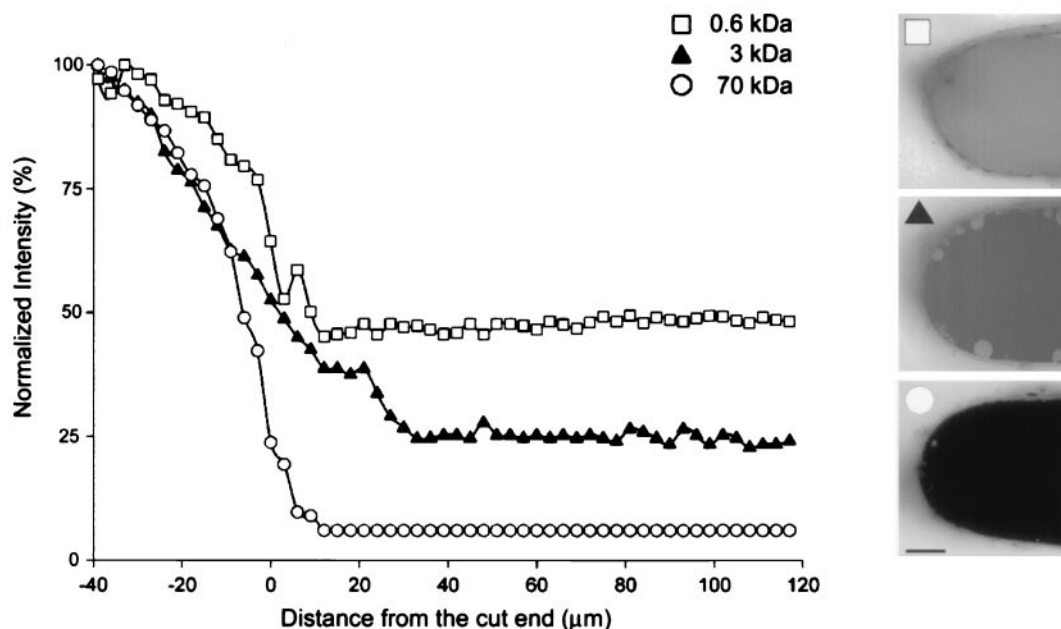
FIGURE 2 Assessments of the exclusion of dye molecules of three different sizes (0.6 kDa, *open squares*, 3 kDa, *closed triangles*, and 70 kDa, *open circles*) at the cut end of three different crayfish MGAs (confocal fluorescence images, cut ends oriented to the left; and scale bar in open circle image = 40 μm for all images) when added to the saline solution bathing each axon at 15 min posttransection. Each confocal image (*right*) was acquired 15 min after dye was added. Graph of fluorescence intensity scans (*left*) of the three images along a line extending from 40 μm outside ($x < 0$) each cut end to 120 μm inside ($x > 0$) each axon. The intensity data for each axon were normalized with respect to their corresponding outside intensity, which was set at 100% for comparison. Notice that the extent of dye exclusion at the same posttransection time depends inversely on the molecular size of the dye. That is, at 15 min posttransection the 70-kDa dye was completely excluded (i.e., a barrier to these large molecules had formed), as indicated by the sharp drop to 7% of the outside intensity over a distance of ± 10 μm, in contrast to the uptake of the smaller 0.6- and 3-kDa dye molecules for which more ($\sim$50% vs. 25%) of the smaller dye molecules (0.6 vs. 3 kDa) had entered.

time posttransection, as would a sieve having a mesh whose diameter decreases with time.

An ionic seal that restores ionic currents to control levels takes longer to form than does a barrier that excludes the smallest dye molecules

To assess the eventual formation of an ionic seal in severed MGAs, we measured at cut axonal ends the temporal decline of a large, inwardly directed I_i with a vibrating probe, and we measured the recovery of E_r (Krause et al., 1994; Eddleman et al., 1997) and propagated action potentials by microelectrode impalement. Before axonal transection, the baseline ionic current density (I_c) was determined by surveying the entire length of each intact axon (see Materials and Methods). After determining individual I_c values in each axon, an average value $\langle I_c \rangle$ for the baseline of all axons ($n = 10$) was calculated and plotted as the dashed line in Fig. 4.

After I_c was determined in an intact MGA, the axon was transected in one of four different solutions (vanH, vanH plus ion channel blockers, divalent-cation-free vanH, Ca^{2+}-free vanH), and I_i was determined at specific posttransection times. The I_i for any given axon, measured 5 min after an MGA was transected, was typically 30$\times$ greater than its

baseline I_c. At the cut end, I_i was maximal and always directed inwardly. As the probe was moved away from the cut end along the length of the axon, I_i was oriented in the direction of the cut end and its intensity diminished progressively. After I_i data were obtained for a number (n) of axons transected in each solution, an average value of I_i was calculated at every posttransection time in that solution. The average $I_i \equiv \langle I_i \rangle$ is plotted in Fig. 4 for different solutions. $\langle I_i \rangle$ in control solution (Fig. 4, *closed circles*) decayed rapidly from 5 to 30 min after transection, and then decayed more slowly (30–70 min). At 60–70 min posttransection, the $\langle I_i \rangle$ for these axons ($n = 10$) was not significantly different ($p < 0.05$) from $\langle I_c \rangle$. This time course for the decay of I_i and $\langle I_i \rangle$ is similar to that reported previously for transected crayfish MGAs and squid GAs transected in solutions containing calpain (Godell et al., 1997) and for transected earthworm MGAs (Krause et al., 1994).

To determine whether conduction in voltage-dependent ion channels affected axonal sealing (George et al., 1995; Sattler et al., 1996) as measured by the decay of the $\langle I_i \rangle$, MGAs were transected in vanH solution containing several blockers of voltage-dependent ion channels (see Materials and Methods) as follows: Na^+ (TTX, [1 μM]), K^+ (TEA, [10 mM] and 4-AP, [1 mM]), Ca^{2+} (nitrendipine, [50 μM]). When MGAs were transected in vanH solution containing
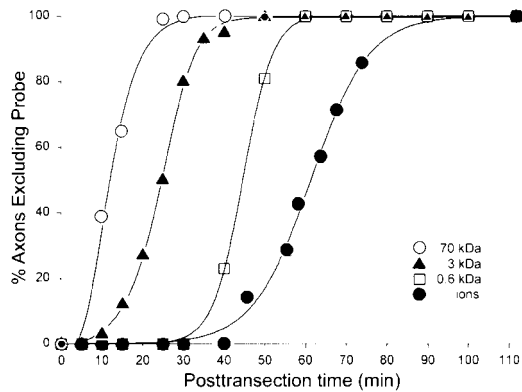
FIGURE 3 The fraction (%) of axons that form a barrier to molecular probes of different size versus posttransection time. The %-axons-excluding-dye versus posttransection-time curves shift progressively to the right (to longer times) as the dye molecular size is decreased from 70-kDa Texas Red-dextran (*open circles*) to 3-kDa Texas Red-dextran (*closed triangles*), and finally to 0.6-kDa Calcein (*open squares*). The posttransection time at which ions were excluded (*closed circles*) was assessed separately by measurement of the temporal decline of I_i to baseline (see Fig. 4). Notice that 1) an ionic seal forms last and only after formation of a barrier to the smallest dye molecule (the principal ions in physiological salines are smaller than the smallest dye molecule tested), 2) none of the curves intersect, and 3) the shape of all curves are very similar.

FIGURE 4 Temporal decline of the average ionic current density ($\langle I_i \rangle$) after transection of MGAs in different saline solutions, measured with a vibrating probe electrode in the extracellular medium at a fixed distance of 150 μm from the disrupted axolemma at the cut end. Initial measurements of I_i in each axon were recorded at 5 min posttransection. Values of I_i acquired at subsequent times posttransection were normalized with respect to the initial I_i determination and expressed as a percentage of the initial value to enable comparison of data from different axons. Each data point is the average ($\langle I_i \rangle$) of the values for percent of initial I_i obtained from all axons at the specific posttransection time. The dashed horizontal line is the average of baseline current densities measured in each uninjured, intact axon before transection. In vanH solution with (*open triangles*, $n = 5$) and without (*closed circles*, $n = 10$) ion channel blockers for Na$^+$, K$^+$, and Ca^{2+} (see text), $\langle I_i \rangle$ decays to baseline in ~65 min after transection. In contrast, in divalent-cation-free vanH ($n = 6$) or Ca^{2+}-free vanH ($n = 10$, *closed squares*), $\langle I_i \rangle$ does not decay to baseline, i.e., an ionic seal does not form. Error bars are ±1 SD.

ion channel blockers (Fig. 4, *open triangles*), the $\langle I_i \rangle$ decayed to $\langle I_c \rangle$, and the time course of the decay was not significantly different compared to the decay of $\langle I_i \rangle$ in the control solution. That is, the $\langle I_i \rangle$ with and without addition of ion channel blockers measured at the same posttransection times were within ±1 SD of each other. In contrast, when MGAs ($n = 16$) were transected in either a divalent-cation-free or a Ca^{2+}-free vanH (see Materials and Methods), the $\langle I_i \rangle$ was *always* very large (Fig. 4) and directed inwardly toward the opening of the cut end. That is, MGAs transected in vanH solutions lacking Ca^{2+} did not restrict ionic entry. Therefore, after transection of MGAs, I_i, as measured in individual axons, and $\langle I_i \rangle$, obtained from an average of the individual I_i data, both decayed monotonically, continuously (without discontinuities), and independently of the conductance of voltage-dependent ion channels.

The decay of I_i to baseline values measured in individual axons and the decay of $\langle I_i \rangle$ calculated from the entire population of axons can be interpreted as the formation of an ionic seal, provided that these axons are not depolarized (electrically dysfunctional) (Krause et al., 1994). To eliminate this alternative possibility, we measured E_r (Table 1) and the ability of axons to propagate action potentials after I_i had decayed to baseline (Table 2). The E_r of intact MGAs was -85 ± 3 (SD) mV. At 5 min posttransection, the E_r measured at the cut end of MGAs was -32 ± 8 mV, i.e., significantly depolarized ($p < 0.05$, Student's *t*-test) compared to intact MGAs. The E_r of transected MGAs whose I_i had decayed to I_c was -84 ± 4 mV, i.e., E_r had recovered to within 5 mV of E_r in intact MGAs (Table 1). Axons
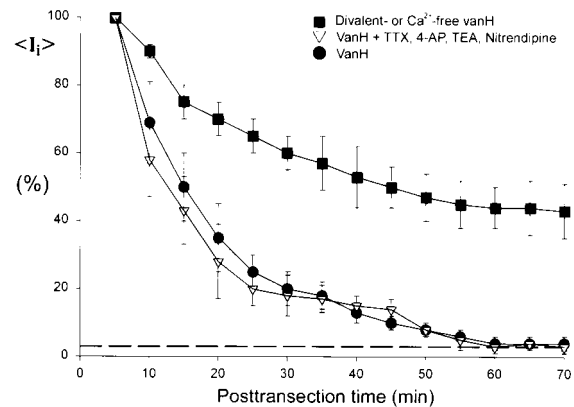
transected and maintained in either divalent-free vanH or Ca^{2+}-free vanH were significantly depolarized and E_r did not recover, as reported previously (Eddleman et al., 1997).

Axons that had an E_r within 5 mV of the uninjured intact axon also could propagate all-or-nothing action potentials (Table 2). The recovery of near normal E_r and action potentials showed that the decay of injury current to baseline was indeed due to the formation of an ionic seal that was sufficient to allow recovery of axonal electrical function.

DISCUSSION

What constitutes a seal, and how should it be assessed?

The exclusion of extracellularly placed hydrophilic, fluorescent dye molecules of various sizes have frequently been

TABLE 1 Recovery of the resting potential (E_r) of MGAs transected in vanH

Pretransection	Posttransection	
E_r (mV) ± SD	Time (min)	E_r (mV) ± SD
-85 ± 3 ($n = 48$)	5	-32 ± 8* ($n = 33$)
	60	-84 ± 4 ($n = 52$)

*Significantly different ($p < 0.05$) from control values.

TABLE 2 Recovery of resting (E_r) and action potentials (APs) in MGAs transected in vanH at posttransection times when I_i is presumed (based on the data in Fig. 4) to have decayed to baseline (I_c)

Pretransection	Posttransection		
E_r (mV)	Time (min)	E_r (mV)	AP (mV)
−89	65	−85	90
−83	71	−80	75
−85	72	−80	76

At 5 min posttransection, E_r typically depolarized to 30 mV (see Table 1) and APs did not propagate within 200 μm of the cut end.

used to determine the existence of a barrier (often called a "seal") after plasmalemmal injury (Xie and Barrett, 1991; Steinhardt et al., 1994; Bi et al., 1995; Terasaki et al., 1997; Eddleman et al., 1998a, b; Blanchette et al., 1999; Lichstein et al., 2000). Previous studies (Eddleman et al., 1998b) have shown that assessments of dye exclusion can depend upon the electrical charge of the dye and other factors (e.g., axoplasmic outflow at the injury site). In addition to these complications in the use of dye to assess barrier formation, our data show that the outcome of dye barrier assessments can also vary depending on the molecular size of the dye used to probe the penetrability of the barrier and the posttransection time at which the assessment is made. More specifically, our data show that a barrier to ionic inflow or outflow (i.e., an ionic seal) is the culmination of an evolving process in which the barrier becomes progressively impermeable to smaller and smaller dye molecules, with the eventual restriction of ionic movements. Dye barrier assessments can provide important information during barrier formation, but they must be combined with other measures (e.g., injury current) to assess whether a dye barrier eventually becomes an ionic seal, which allows recovery of resting and action potentials.

Ionic sealing is unaffected by the state of conduction in axolemmal ion channels

Because axolemmal ion channels are necessary for axonal electrical activity and also serve many other axonal functions, they might also have a role in axonal sealing after injury. For example, elevation of the axoplasmic concentration of Ca^{2+} is necessary for the initiation of vesiculation, leading to axonal repair, and the degradation of axonal proteins, leading to axonal degeneration. Ca^{2+} could enter axons from extracellular fluid through voltage-dependent ion channels in an otherwise-undamaged axolemma (George et al., 1995; Sattler et al., 1996), rather than by inflow at cut axonal ends where accumulated vesicles form a barrier. Our data showing that the time course of ionic sealing, as reflected in the decay of I_i to baseline, is not affected by ion channel blockers are consistent with a hy-

pothesis that increases in internal Ca^{2+} result from Ca^{2+} inflow at the cut end (Eddleman et al., 1998a; Bittner and Fishman, 2000), rather than Ca^{2+} inflow across ion channels in the axolemma. This conclusion is consistent with other data showing that Ca^{2+} inflow at the cut end best accounts for temporal changes in fluorescent Ca^{2+} indicators in severed squid (Fishman et al., 1995), lamprey (Strautman et al., 1990), and *Aplysia* (Ziv and Spira, 1995) axons.

Does a single barrier whose properties change with time seal severed axons?

Many properties of barrier formation in severed axons are consistent with the gradual formation of a single barrier (not necessarily a single membranous sheet) with time-varying characteristics.

First, in the present experiments, optical measures show a progressive exclusion at axonal cut ends of dye molecules of decreasing size (Fig. 3). The curves for the exclusion of all dye molecules are similarly shaped and do not intersect.

Second, electrical measures showing a continuous and smooth decay of I_i (Godell et al., 1997) or $\langle I_i \rangle$ to baseline (Fig. 4, *closed circles*) also yield a curve for ionic exclusion at axonal cut ends that has a similar shape to dye exclusion curves and does not intersect them when plotted on the same axes (Fig. 3). This similar and progressive change of permeability with time in independent optical and electrical measures (Fig. 3) is consistent with the formation of a single barrier. As expected for a single barrier, the exclusion of different-sized molecules by the developing barrier proceeds successively from the largest to the smallest molecule and ends with the exclusion of ions, which are smaller than any dye molecule. Conversely, once an ionic barrier is complete (an ionic seal), this barrier always is impenetrable by dye molecules whose size is larger than ions found in the intracellular or extracellular media.

Third, previous reports of dye barriers in severed giant axons are also consistent with the formation of a single barrier with time-variant characteristics. For example, the fluorescence boundary marking dye exclusion (determined by confocal microscopy) is located amid an accumulation of vesicles at the cut end (Eddleman et al., 1997, 1998a). The magnitude of the I_i vector (determined from vibrating probe measures) is maximal at the cut end, and the vector is directed inwardly toward the cut end (Krause et al., 1994; Godell et al., 1997). Furthermore, when individual MGAs are filled with hydrophilic, fluorescent dye molecules of different size and viewed in time-lapse confocal images, the configuration and location of the dye barrier changes continuously from 15 to 35 min posttransection (or exposure of cut axonal ends to Ca^{2+}) and then stabilizes (Blanchette et al., 1999; Lichstein et al., 2000). Once formed, the location and configuration of the moving dye barrier is the same for dye molecules of different size at all times after transection
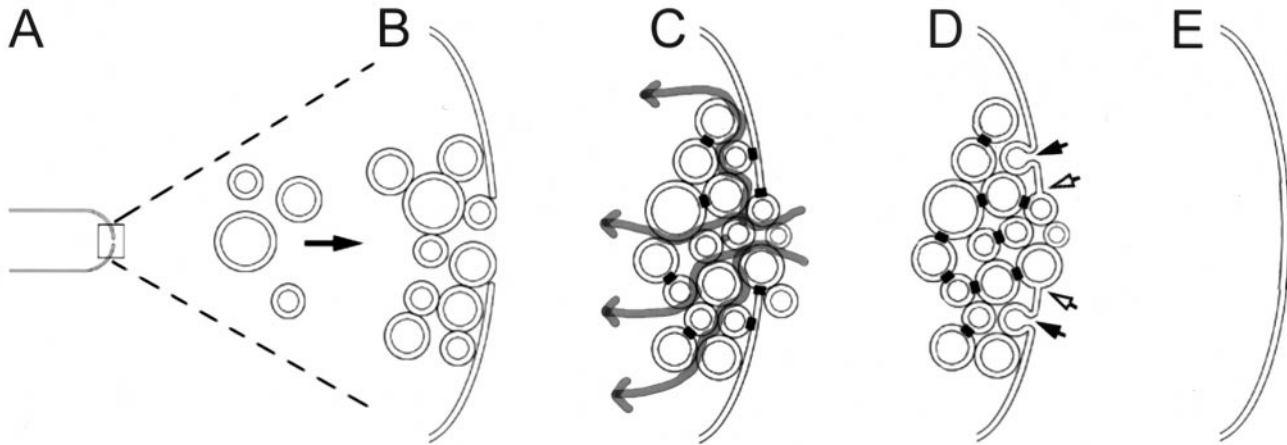
FIGURE 5 Diagram of vesicle-mediated formation of an ionic seal at the cut end of an axon, which accounts for the slow, gradual transition from a barrier that progressively excludes molecules of decreasing size to one that eventually restricts ionic movements. (*A*) After transection of a crayfish MGA, vesicles induced by elevated Ca^{2+} form by endocytosis of the axolemma and move to the partially collapsed (*box*) cut end (Eddleman et al., 1998a). (*B*) Vesicles accumulate and become densely packed at the disrupted portion of axolemma (Eddleman et al., 1997). (*C*) Vesicle membranes interact with each other and the axolemma and some form junctional complexes (*black dots joining adjacent membranes*) (Eddleman et al., 1997) that decrease both the number and conductance of paths (*contorted dark lines with arrowheads*) for ion entry into or exit from the axolemmal disruption. (*D*) An ionic seal has formed (i.e., ionic conduction through the disrupted portion of axolemma has been reduced to the level in the intact axolemma). Reestablishment of axolemmal continuity begins or has begun either directly by vesicle fusions with the boundary of the disrupted axolemma (*between open arrows*) and/or indirectly by fusion with the intact portion of axolemma (*closed arrows*). (*E*) At a substantial time after an ionic seal is formed (≫60 min), axolemmal continuity is restored and vesicles are no longer evident (Lichstein et al., 2000).

or exposure of cut axonal ends to Ca^{2+}. Finally, in the first 5–15 min after transection, when dye barriers are not yet formed and/or are in the process of being formed, the transition from no dye barrier to a dye barrier is not abrupt (e.g., Fig. 3, *A--C* of Lichstein et al., 2000).

The transformation of a barrier to dye molecules into an ionic seal

Our data showing an inverse relationship between the size of the molecular probe and the posttransection time at which 100% of the axons exclude the probe strongly suggest that a barrier to large dye molecules forms within minutes of transection at cut axonal ends, but that the transformation of this barrier into an ionic seal is a gradual, much slower process requiring an hour or more for completion. The lack of an abrupt, large change in barrier permeability is inconsistent with a sudden reestablishment of axolemmal continuity, e.g., by the collapse and fusion of severed axolemmal leaflets, which is the conventional explanation of axonal sealing (Kandel et al., 1997). Although this lack of a collapse of axonal cut ends could be attributed to differences between giant and smaller axons, no convincing evidence of a complete collapse has been reported for small axons. Furthermore, severed neurites (~1 μm in diameter) of cultured neurons require relatively long times (15–20 min) to form a dye barrier (Detrait et al., 2000). In contrast, none of the giant axons from four different invertebrates [cockroach (Yawo and Kuno, 1985), crayfish (Eddleman et al., 1997, 1998a), earthworm (Krause et al., 1994), and squid (Krause

et al., 1994)] has been observed to collapse, i.e., a significant opening always persists at the cut end. This opening is typically filled with vesicles that form at, and or migrate to, the cut end (Krause et al., 1994; Eddleman et al., 1997, 1998a; Ballinger et al., 1997; Lichstein et al., 2000). Without a complete collapse of the axolemma at a cut end, the disrupted portions of axolemma would be very unlikely to fuse to immediately reconstitute an intact axolemma, and thereby immediately form a complete ionic seal. Alternatively, vesicles that accumulate and continuously interact (pack more tightly, form complexes, and/or fuse) at a site of axolemmal damage (Eddleman et al., 1997, 1998a) could account for a barrier that progressively and gradually restricts the inflow or outflow of dye molecules of decreasing size and, eventually, ions. Vesicles have also been reported to seal, within seconds, punctures or larger disruptions of the plasmalemmal membrane of oocytes, possibly by fusion of cortical granules (Steinhardt et al., 1994) or "patch vesicles" (Terasaki et al., 1997; McNeil et al., 2000) with the intact portion of plasmalemmal membrane. Such mechanisms should be associated with sudden and discontinuous changes in dye exclusion or I_i, similar to that expected for collapse and fusion of axolemmal leaflets (Kandel et al., 1997) and should yield data at variance with that reported here for repair of axolemmal damage. Furthermore, the disparity in the time necessary to form an ionic barrier in an injured axon compared to that required to repair a disrupted oocyte plasmalemma cannot be attributed to the size or type of injury, because small punctures in crayfish axolemma (comparable to those in oocytes repair studies) have been

reported to take a relatively long time (minutes) to seal (Eddleman et al., 1998a).

To summarize and integrate all these data, we envisage the repair of axolemmal damage to be mediated by vesicles as illustrated in Fig. 5. Initially (Fig. 5 *A*), vesicles that form after injury by Ca^{2+}-induced endocytosis of the axolemma (Eddleman et al., 1998a), accumulate and densely pack at the cut end (Fig. 5 *B*). The membranes of these vesicles then interact with each other and the intact axolemma to form complexes (Fig. 5 *C*) (Eddleman et al., 1997) that decrease both the number and ionic conduction of pathways (from outside the axon to its interior through the occluding vesicular mass) by the progressive diminution of the interstitial fluid between vesicles, which in turn reduces the permeation of dye molecules of decreasing size. Finally, ionic conduction through the vesicular accumulation is reduced to an extent that an ionic seal is established (Fig. 5 *D*) which allows recovery of electrical function (resting and action potentials). During and/or after formation of an ionic seal (Fig. 5 *D*), vesicle fusions with the plasma membrane are mediated by fusion-promoting proteins (Detrait et al., 2000) at the disrupted boundary of the axolemma (*between open arrows*, Fig. 5 *D*) and/or with the intact axolemma (*closed arrows*, Fig. 5 *D*) (Eddleman et al., 1997; Bittner and Fishman, 2000). Vesicle-membrane fusions continue until the vesicles are consumed and axolemmal continuity is reestablished (Fig. 5 *E*), many hours after an ionic seal has formed (Lichstein et al., 2000).

REFERENCES

Ballinger, M., and G. D. Bittner. 1980. Ultrastructural studies of severed giant and other CNS axons in crayfish. *Cell Tissue Res.* 208:123–133.

Ballinger, M. L., A. R. Blanchette, T. L. Krause, M. E. Smyers, H. M. Fishman, and G. D. Bittner. 1997. Delaminating myelin membranes help seal the cut ends of severed earthworm giant axons. *J. Neurobiol.* 33:945–960.

Bi, G., J. M. Alderton, and R. A. Steinhardt. 1995. Calcium-regulated exocytosis is required for cell membrane resealing. *J. Cell Biol.* 131: 1747–1758.

Bittner, G. D., and H. M. Fishman. 2000. Axonal sealing following injury. *In* Nerve Regeneration. N. Ingoglia and M. Murray, editors. Marcel Dekker, New York. 337–369.

Blanchette, A. R., M. L. Ballinger, H. M. Fishman, and G. D. Bittner. 1999. Calcium entry initiates processes that restore a barrier to dye entry in severed earthworm axons. *Neurosci. Lett.* 272:147–150.

Detrait, E., S. Yoo, C. S. Eddleman, M. Fukuda, G. D. Bittner, and H. M. Fishman. 2000. Plasmalemmal repair of severed neurites of PC12 cells requires Ca^{2+} and synaptotagmin. *J. Neurosci. Res.,* in press.

Detrait, E., C. S. Eddleman, S. Yoo, M. Fukuda, M. P. Nguyen, G. D. Bittner, and H. M. Fishman. 2000. Axolemmal repair requires proteins that mediate synaptic vesicle fusion. *J. Neurobiol.* 44:382–391.

Eddleman, C. S., M. L. Ballinger, C. M. Godell, M. E. Smyers, H. M. Fishman, and G. D. Bittner. 1997. Repair of plasmalemmal lesions by vesicles. *Proc. Natl. Acad. Sci. USA.* 94:4759–4764.

Eddleman, C. S., M. L. Ballinger, M. E. Smyers, H. M. Fishman, and G. D. Bittner. 1998a. Endocytotic formation of vesicles and other membranous structures induced by Ca^{2+} and injury. *J. Neurosci.* 18:4029–4041.

Eddleman, C. S., M. E. Smyers, A. L. Lore, H. M. Fishman, and G. D. Bittner. 1998b. Anomalies associated with dye exclusion as a measure of axolemmal repair in invertebrate axons. *Neurosci. Lett.* 256:123–126.

Fishman, H. M., T. L. Krause, A. L. Miller, and G. D. Bittner. 1995. Retardation of the spread of extracellular Ca^{2+} into transected, unsealed squid giant axons. *Biol. Bull.* 189:208–209.

George, E. B., J. D. Glass, and J. W. Griffin. 1995. Axotomy-induced axonal degeneration is mediated by calcium influx through ion-specific channels. *J. Neurosci.* 15:6445–6452.

Godell, C. M., M. E. Smyers, C. S. Eddleman, M. L. Ballinger, H. M. Fishman, and G. D. Bittner. 1997. Calpain activity promotes sealing of severed giant axons. *Proc. Natl. Acad. Sci. USA.* 94:4765–4770.

Jaffe, L. F., and R. Nuccitelli. 1974. An ultrasensitive vibrating probe for measuring steady extracellular currents. *J. Cell Biol.* 63:614–628.

Kandel, E. R., J. H. Schwartz, and T. M. Jessell. 1997. Essentials of Neural Science and Behavior. Appleton and Lange, Norwalk, CT.

Krause, T. L., H. M. Fishman, M. L. Ballinger, and G. D. Bittner. 1994. Extent and mechanism of sealing in transected giant axons of squid and earthworms. *J. Neurosci.* 14:6638–6651.

Lichstein, J. W., M. L. Ballinger, A. R. Blanchette, H. M. Fishman, and G. D. Bittner. 2000. Structural changes at cut ends of earthworm giant axons in the interval between dye barrier formation and neuritic outgrowth. *J. Comp. Neurol.* 416:143–157.

McNeil, P. L., S. S. Vogel, K. Miyake, and M. Terasaki. 2000. Patching plasma membrane disruptions with cytoplasmic membrane. *J. Cell Sci.* 113:1891–1902.

Narahashi, T. 1974. Chemicals as tools in the study of excitable membranes. *Physiol. Rev.* 54:813–889.

Sattler, R., M. Tymianski, I. Feyaz, M. Hafner, and C. H. Tator. 1996. Voltage-sensitive calcium channels mediate calcium entry into cultured mammalian sympathetic neurons following neurite transection. *Brain Res.* 719:239–246.

Scheffey, C. 1988. Two approaches to construction of vibrating probes for electrical current measurement in solution. *Rev. Sci. Instrum.* 5:787–792.

Steinhardt, R. A., G. Bi, and J. M. Alderton. 1994. Cell membrane resealing by a vesicular mechanism similar to neurotransmitter release. *Science.* 263:390–393.

Strautman, A. F., R. J. Cork, and K. R. Robinson. 1990. The distribution of free calcium in transected spinal axons and its modulation by applied electrical fields. *J. Neurosci.* 10:3564–3575.

Terasaki, M., K. Miyake, and P. McNeil 1997. Large plasma membrane disruptions are rapidly resealed by Ca^{2+}-dependent vesicle-vesicle fusion events. *J. Cell Biol.* 139:63–74.

van Harreveld, A. 1936. A physiological solution for freshwater crustaceans. *Proc. Soc. Exp. Biol. Med.* 34:428–432.

Xie, X., and J. N. Barrett. 1991. Membrane resealing in cultured rat septal neurons after neurite transection: evidence for enhancement by Ca^{2+}-triggered protease activity and cytoskeletal disassembly. *J. Neurosci.* 11:3257–3267.

Yawo, H., and M. Kuno. 1985. Calcium dependence of membrane sealing at the cut end of the cockroach giant axon. *J. Neurosci.* 5:1626–1632.

Ziv, N. E., and M. E. Spira. 1995. Axotomy induces a transient and localized elevation of the free intracellular calcium concentration to the millimolar range. *J. Neurophysiol.* 74:2625–2637.